Fish and Shellfish Immunology 92 (2019) 667–679

Contents lists available at ScienceDirect

Fish and Shellfish Immunology

journal homepage: www.elsevier.com/locate/fsi

Full length article

A histone H2A derived antimicrobial peptide, *Fi*-Histin from the Indian White shrimp, *Fenneropenaeus indicus*: Molecular and functional characterization

K.S. Sruthy[a], Aishwarya Nair[a], Swapna P. Antony[a], Jayesh Puthumana[b], I.S. Bright Singh[b], Rosamma Philip[a,*]

[a] Department of Marine Biology, Microbiology and Biochemistry, School of Marine Sciences, Cochin University of Science and Technology, Fine Arts Avenue, Kochi, 682016, Kerala, India

[b] National Centre for Aquatic Animal Health, Cochin University of Science and Technology, Kochi, 682016, Kerala, India

ARTICLE INFO

Keywords:
Antimicrobial peptide
Histone H2A
Fenneropenaeus indicus
Synthetic peptide
Anticancer activity

ABSTRACT

Antimicrobial peptides (AMPs) derived from histone proteins form an important category of peptide antibiotics. Present study deals with the molecular and functional characterization of a 27-amino acid histone H2A derived AMP from the Indian White shrimp, *Fenneropenaeus indicus* designated as *Fi*-Histin. This peptide displayed distinctive features of AMPs such as amphiphilic alpha helical structure and a net charge of +6. The synthetic peptide exhibited significant antimicrobial activity against Gram-negative and Gram-positive bacteria especially against *V. vulnificus*, *P. aeruginosa, V. parahaemolyticus, V. cholera* and *S. aureus*. Disruption of cell membrane and cell content leakage were observed in peptide treated *V. vulnificus* using scanning electron microscopy. The synthetic peptide *Fi*-His_{1-21} exhibited DNA binding activity and found to be non-haemolytic at the tested concentrations. Peptide was also found to possess anticancer activity against NCI–H460 and HEp-2 cell lines with an IC_{50} of 22.670 ± 13.939 μM and 31.274 ± 24.531 μM respectively. This is the first report of a histone H2A derived peptide from *F. indicus* with a specific antimicrobial activity and anticancer activity, which could be a new candidate for future applications in aquaculture and medicine.

1. Introduction

In the current scenario of emergence of multidrug resistant pathogens and malignancy, antimicrobial peptides (AMPs) would be a potential alternative to conventional antibiotics and cancer therapeutics [1–4]. AMPs are produced in active form after proteolytic cleavage of precursor proteins/peptides that are pre-arranged by the host genome and ribosomally synthesized. These are short peptides (10–100 amino acids) with a net positive charge (+2 to +9) and considerable proportion (> 30%) of hydrophobic residues [5]. Most of the peptides either fold into an amphipathic α-helix and/or β-sheet structures upon contact with anionic microbial membranes. Histones are the integral protein part of chromatin which is involved in various biological activities [6]. Histone proteins are primarily engaged in the packing of genomic DNA, fundamentally aiding the folding of extensive DNA strands to a coin like manner and transcription regulation [7]. Eukaryotic nuclei is mainly comprised of histone proteins and this includes the nucleosome with core histones encompassing H2A, H2B, H3 and H4 and the linker histones containing H1 and H5 proteins. Histone proteins are also highly alkaline peptides rich in Lys/Arg residues, which make them potent antimicrobial agents against negatively charged cell membranes. Among which, histones H1, H2A, and H2B are rich in Lys residues whereas H3 and H4 are rich in Arg residues [8].

Histones play a major role in the nucleus and can also act as antimicrobials against invading pathogens. For the first time Kim and coworkers identified and characterized a 39 amino acid residue histone derived antimicrobial peptide (HDAP) named, buforin I from the stomach tissue of Asian toad, *Bufo gargarizans* [9]. Later in the same year Park et al. [10] identified a 21 amino acid peptide named buforin II, exhibiting broad spectrum antimicrobial activity with no haemolytic activity. Using synthetic buforin II labelled with FITC, the mechanism of antimicrobial activity was revealed and found to be non-membrane lytic mode of killing *via* interaction with nucleic acid [11]. A few studies regarding antimicrobial activity of HDAPs have been reported from invertebrates, including histone H2A fragments in scallop (*Chlamys farreri*) [12], abalone (*Haliotis discus discus*) [13], Pacific white shrimp

* Corresponding author.
E-mail addresses: rosammap@gmail.com, rose@cusat.ac.in (R. Philip).

https://doi.org/10.1016/j.fsi.2019.06.044
Received 16 January 2019; Received in revised form 22 June 2019; Accepted 23 June 2019
Available online 26 June 2019

(*L. vannamei*) [14], freshwater prawn (*M. rosenbergii*) [15,16] and mud crab *S. paramamosain* [17]. In addition to antimicrobial activity, the HDAPs also exhibited potent anticancer activity [18]. Among the HDAPs, buforinIIb, the synthetic analogue of buforin II was found to aim cancer cells selectively by interacting with the cell-surface gangliosides and was found to be able to pass through cancer cell membranes (without damaging) effecting mitochondria-dependent apoptosis [19]. Another reported HDAP from disk abalone (*H. discus discus*), abhisin, a potential AMP derived from histone H2A, also showed antimicrobial and anticancer activity similar to that of buforinIIb [13].

To date only few H2A derived AMPs are reported from shrimp species. In the past decade only a few AMPs have been reported from the Indian white shrimp, *Fenneropenaeus indicus* including isoforms of crustins [20,21] and penaeidins [22,23]. In the present study, a histone H2A derived AMP has been identified from *F. indicus* (*Fi*-Histin) and to unveil its biological activity, the peptide was custom synthesized as a linear peptide. Antimicrobial and anticancer activities of the synthetic peptide were tested. Toxicity was tested by haemolytic assay. This study would help exploring the possibilities of utilizing the histone derived peptides for therapeutic applications.

2. Materials and methods

2.1. Details of the experimental organism and haemolymph collection

Live and healthy Indian white shrimp, *Fenneropenaeus indicus* was collected from Cochin estuary along Fort Kochi, Kerala, India. The samples were taken to the laboratory in live condition by providing proper aeration. Using DEPC treated RNase-free capillary tubes rinsed using pre-cooled anticoagulant solution (RNase free 10% sodium citrate, pH 7.0 in DEPC treated water), haemolymph was collected from rostral sinus of *F. indicus*. Haemolymph was homogenised in TRI reagent (Sigma) using RNase free micro-pestle and kept at −20 °C for total RNA isolation.

2.2. RNA extraction and reverse transcription

Total RNA was extracted from haemolymph in accordance with the TRI reagent (Sigma) specification. The first strand cDNA was synthesized in a 20 μL reaction volume containing 5 μg total RNA, 1x RT buffer, 2mM dNTP, 2 mM oligo d(T20), 20U of RNase inhibitor, and 100U of MMLV reverse transcriptase (New England Biolabs, USA). The reaction was incubated at 42 °C for 1 h followed by an inactivation step at 85 °C for 15 min. Beta-actin was used as an internal control to verify the RT-PCR reaction.

2.3. PCR amplification and TA cloning

The product from reverse transcription, single strand cDNA was used as the template to amplify the house-keeping gene, beta-actin with gene-specific primers (Table 1). After confirmation, the cDNA was used to amplify HDAP, with Hipposin primers [24] in a 25 μl reaction volume containing 1X standard Taq buffer (10 mM TrisHCl, 50 mM KCl, pH 8.3), 3.5 mM $MgCl_2$, 200 μM dNTPs, 0.4 μM each primer and 1U Taq DNA polymerase. The PCR condition was 95 °C for 2 min followed by 35 cycles of 94 °C for 15 s, 60 °C for 30 s and 72 °C for 30 s and a final extension at 72 °C for 10 min. Amplicons were cloned into pGEM®-T Easy cloning vector (Promega) and transformed using competent *E. coli* cells, DH5α as per manufacturer's protocols. Recombinant clones were selected by blue/white screening and single white colonies were cultured overnight for plasmid extraction. Plasmid DNA was purified using GenEluteHp Plasmid Miniprep Kit (Sigma) and sequenced using T7F and SP6R primers on an ABI Prism 377 DNA sequencer (Applied Biosystem) at SciGenom Sequencing Facility, India.

2.4. Bioinformatics analysis

Expert Protein Analysis System (ExPASy) translate tool (http://au.expasy.org/translate) was used to deduce amino acid sequence from the nucleotide sequence. Homology of nucleotide and deduced amino acid sequences were performed using BLASTn and BLASTp algorithm of the NCBI (http://www.ncbi.nlm.nih.gov/blast). Physico-chemical parameters of the peptide were predicted separately using the online protein parameters analysis tool, ExPASy PROTPARAM bioinformatics resource portal (http://web.expasy.org/protparam) and Protein calculator (http://protcalc.sourceforge.net/). To evaluate the segregation of hydrophobic and hydrophilic amino acid residues in the peptide, helical property prediction was done using Heliquest online tool (http://heliquest.ipmc.cnrs.fr/cgi-bin/ComputParamsV2.py). Hydrophobic nature of the peptide was analysed using the Kytee-Doolittle plot using the ProtScale tool of ExPASy bioinformatics resource portal (http://web.expasy.org/protscale).

The antimicrobial activity was predicted using *in silico* using Antimicrobial peptide database – calculation and prediction tool (http://aps.unmc.edu/). Multiple sequence alignment of deduced amino acid sequence of peptide with other histone H2A derived AMP encoding sequences was conducted using ClustalW in BioEdit software for the comparison and alignment. The phylogenetic tree was constructed using Neighbor-Joining method using MEGA version 7.0. The cDNA sequence of peptide was converted to the corresponding RNA sequence (http://www.attotron.com/) and submitted to RNA Fold Server Program (http://rna.tbi.univie.ac.at/cgi-bin/RNAfold.cgi) to visualize the RNA structure with minimum free energy (MFE) to observe the stability of mRNA structure. Using the SWISS-MODEL prediction algorithm based on homology modelling, the spatial structure was established with PyMOL [26]. The secondary structure prediction of the peptide was also analysed and confirmed using PSIPRED protein sequence analysis work bench (http://bioinf.cs.ucl.ac.uk/psipred/). The nucleotide sequence and deduced amino acid sequence of *Fi*-Histin were submitted to GenBank.

2.5. Peptide synthesis and characterization

Chemical synthesis of the peptide with FITC labelling was carried out at M/s Zhejiang Ontores Biotechnologies Co., Ltd China by Solid phase procedure of Fmoc chemistry with > 95% final purity. Peptide synthesis was performed from N to C terminus with end modifications including N- terminus acetylation and C-terminus amidation. Linear synthetic peptide supplied as lyophilized powder was solubilised in sterile water and stored at −20 °C for further use.

Table 1
Primer sequence and details of primers used.

Target gene	Sequence (5′-3′)	Product Size (bp)	Annealing Temp. (°C)	$MgCl_2$ Conc. (mM)
Hipposin	F: ATGTCCGGRMGMGGSAARAC R:GGGATGATGCGMGTCTTCTTGTT	81	55	1.5
β-actin	F:CTTGTGGTTGACAATGGCTCCG R: TGGTGAAGGAGTAGCCACGCTC	520	60	1.5

2.6. Mass spectrometry analysis of synthetic peptide

Mass spectrometry was performed at Zhejiang Ontores Biotechnologies Co., Ltd, China to verify the molecular mass and quality of peptide. The spectra analysis was performed with a ThermoFinnigan LCQ Duo mass spectrometer with an electrospray source and Xcaliber software. Synthetic peptide was reconstituted in 50% acetonitrile and 50%, 0.1% trifluoroacetic acid (v/v) and analysed using Electrospray Ionization (ESI) probe with a probe bias of −3.5kv and the nebulizer gas flow maintained at 1.5 L/min. The spectra were obtained by scanning from 400 to 2000 *m/z* at a scan time of 5 s.

2.7. Purity determination of synthetic peptide using HPLC

The homogeneity of the synthetic peptide was determined using HPLC (at Zhejiang Ontores Biotechnologies Co., Ltd, China). Synthetic peptide was dissolved in 50 μl of 0.1% trifluoroacetic acid (TFA) and 10 μl of the sample was injected to the Inertsil ODS-SP column of dimensions 4.6 mm × 250 mm. A step gradient system of solvents were used for purification; beginning with a solvent gradient of 27% Solvent A (0.1% TFA in 100% acetonitrile) and 73% solvent B (0.1% TFA in 100% H_2O) for 0.01 min, followed by a gradient of 52% solvent A and 48% solvent B for 25 min and finally a flow of 100% solvent A for 25 min.

2.8. Haemolytic effect of peptide

Haemolytic assay was performed as described by Onuma et al. [25] with minor modifications using human RBCs (hRBCs). Briefly, the hRBCs were centrifuged at 3000 × *g* for 15 min at 4 °C. The cells were washed with equal volume of phosphate buffer saline (35 mM phosphate buffer, 150 mM NaCl (pH 7.2)) until the colour of the supernatant turned clear. The hRBCs 4% (v/v) suspended in PBS was mixed with different concentrations of peptide (3.125–400 μM) by two fold dilution, incubated for 1 h at 37 °C without agitation and centrifuged at 5000 × *g* for 5 min. The supernatants were collected and transferred to 96 well plates and absorbance was measured at405 nm to examine haemoglobin release. Phosphate buffered saline and Triton X-100 were used to determine zero haemolysis (negative control) and 100% haemolysis (positive control) respectively. Percentage haemolysis was calculated by the following formula: Percentage haemolysis = 100 $[(A_s - A_0)/(A_t - A_0)]$; where A_s represents absorbance of peptide treated sample at 405 nm and A_0 and A_t represent zero % and 100% haemolysis.

2.9. Antimicrobial activity

In brief, eleven types of bacteria (Gram positive bacteria: *B. cereus* and *S. aureus*; Gram negative bacteria: *E. tarda, P. aeruginosa, A. hydrophila, E. coli*, *V. cholera, V. vulnificus, V. proteolyticus, V. alginolyticus* and *V. parahaemolyticus*) were used for the study.

2.9.1. Determination of minimum inhibitory concentration and minimum bactericidal concentration of the synthetic peptide

The MIC of synthetic peptide was determined by broth microdilution method with slight modifications [26]. Dilution series of the synthetic peptide (50–3.125 μM concentrations) were prepared and used for antimicrobial assay. Concisely, 10 μl each of the peptide (various dilutions) was incubated with 10 μl of a suspension of mid-logarithmic phase bacteria (10^6 cfu/ml in 50 mM 4-(2-hydroxyethyl)-1-piperazine ethane sulfonic acid (HEPES) buffer pH 7.4) in a sterile 96 well microtiter plate and incubated at room temperature for 2 h. Then Muller Hinton broth (MH broth) was added to each well and incubated for an additional 24 h at 37 °C with shaking at 100 rpm. Microbial growth was determined by measuring absorbance at 600 nm after 24 h incubation. Inhibition was calculated as follows: Inhibition % = 100 – Growth percentage. Where, Growth % = (OD of Test/OD of Control) * 100. The inhibition percentage was calculated as the average of three independent experiments performed in triplicate.

The bactericidal effect of the peptide was also determined according to Andra et al. [27] with minor modifications. After incubation of the pathogens with the peptide as described above, aliquot of 50 μl was taken and plated on to MH agar plates. Plates were incubated overnight at 37 °C and the colonies were counted. The minimal bactericidal concentration (MBC) of peptide for a given bacterial strain was considered as the lowest concentration of the peptide which could prevent any residual colony formation following incubation for 24 h at the suitable temperature [28].

2.9.2. Propidium iodide staining

To confirm the interaction of the peptide with pathogens, microscopic observation of peptide treated pathogens were done using epifluorescence microscopy after propidium iodide (PI) staining. Briefly, pathogens which were found sensitive against the peptide were treated at the MIC and incubated at 37 °C for 2 h without shaking and cells were collected by centrifugation at 10000 rpm for 5 min, re-suspended and washed in PBS. Bacterial pellet was re-suspended in 200 μl of PI solution (50 μg/mL (in PBS)), mixed well, incubated at room temperature in dark for 5 min, bacterial pellet was collected by centrifugation, washed twice in PBS and smear was prepared for observation. Images were examined using a filter with excitation wavelength of 540–580 nm and an emission filter of 600–660 nm under a Fluorescence microscope (Leica DMRA, Heidelberg, Germany) and photographed within 30 min with a Leica DMDL digital camera. Since the peptide is FITC labelled, the fluorescence of FITC was visualized using a filter with an excitation and emission wavelength of 495 nm/519 nm.

2.9.3. Detection of morphological changes by scanning electron microscopy

Log phase culture of bacteria was incubated with the synthetic peptide (at MIC) at 37 °C for 30 min and bacterial pellet was collected by centrifugation at 10000 rpm for 5 min, re-suspended and washed with 0.1 M sodium phosphate buffer. Cultures without peptides were used as negative control. Then bacterial cells were pre-fixed in 2.5% glutaraldehyde at room temperature for 2 h, fixed in 1% osmium tetroxide at 4 °C for 2 h and dehydrated in graded series of ethanol (50%, 70%, 90%, 95%, and 100%). Bacterial cells were air dried after immersion in hexamethyldisilazane (Sigma) for 20 min and sputter coated with gold in an ion coater, and subjected to morphological observation using a VEGA3 TESCAN scanning electron microscope.

2.10. DNA binding assay

The DNA binding activity of the synthetic peptide was examined using pUC-18 plasmid DNA by a gel retardation assay with slight modification as described by Park et al. [29]. In brief, increasing concentrations of peptide and 50 ng of pUC-18 plasmid DNA were incubated at room temperature in a peptide to DNA ratio of 0:1, 2.5:1, 5:1, 10:1, 20:1 and 50:1 in 20 μl of binding buffer (5% glycerol, 10 mM Tris–HCl (pH 8.0), 1 mM EDTA, 1 mM DTT, 20 mM KCl and 50 μg/ml BSA) for 1 h. Plasmid DNA bands were analysed by electrophoresis in 1.5% agarose gel in Tris Borate-EDTA (TBE) buffer stained with ethidium bromide and visualized under UV light.

2.11. Anticancer activity

2.11.1. In vitro cytotoxicity assay

Human lung cancer cell line NCI–H460 and human laryngeal carcinoma cell line HEp-2 cell lines purchased from National Centre for Cell Science (NCCS, Pune) were employed to assess the inhibitory effect of peptide on cellular metabolism. XTT assay was used to determine the cytotoxic effect of synthetic peptide in NCI–H460 and HEp2 cell lines. Succinate-tetrazolium reductase enzyme system involved in the

mitochondrial respiratory chain reduces XTT to a water soluble formazan yielding an orange coloured solution, which is directly proportional to the cell viability.

About, 1×10^6/ml of cells were inoculated into each well of a 96 well tissue culture plate containing RPMI 1640 medium and incubated for 12 h at 37 °C. After incubation, the cells were washed twice with phosphate buffered saline (PBS), and the medium was exchanged with fresh RPMI 1640 medium containing desired concentrations of the peptide (two fold serial dilutions) and incubated for 24 h at 37 °C. The medium was changed and 50 µl of 2, 3-bis [2-methyloxy-4-nitro-5-sulfophenyl]-2H-tetrazolium-5-carboxanilide (XTT) solution (1 mg/ml in RPMI 1640 medium with 25 µl PMS solution (3 mg PMS into 1 mL PBS)) was added and incubated for 2 h at 37 °C in a CO_2 incubator. The absorbance was measured using a Microplate Reader (TECAN Infinite Tm, Austria) at 450 nm with 690 nm as reference and the difference was calculated. The IC_{50} was calculated as the concentration of peptide that induced 50% growth inhibition with respect to the untreated control.

2.11.2. Gene expression analysis using real-time reverse-transcription polymerase chain reaction (RT-PCR)

To evaluate the anticancer activity of the synthetic peptide, the NCI–H460 cell lines and HEp2 cell lines were incubated in DMEM supplemented with 10% FBS and antibiotic mixture (1% penicillin-streptomycin) in the presence of 25 µM and 50 µM of the peptide for 24 h. Cells incubated without peptide was treated as the control. After incubation, the cells were suspended in TRI reagent (Sigma) for RNA isolation and single stranded cDNA was synthesized from total RNA. A real-time RT-PCR analysis was used to understand the effect of peptide on the cell function post treatment with the peptide by analysing the gene expression pattern of twenty three genes *viz.*, Bcl-2, Bax, Caspase-3, Caspase-9, Cathepsin-G, Calpain-5, Rb1, p-53, Akt1, MAPK-1, JNK, IL-1β, IL-2, IL-6, IL-10, IL-12, IFN-β, IFN-γ, TNF-α, viperin, MX1, ISG15 and IFITM3 (Table 2). GAPDH was used as the reference gene (Table 2).

The SYBR® Green PCR Master Mix (ABI, USA) and specific primer pairs were used for the selected genes. Quantitative real time PCR (qRT-PCR) was performed in StepOne Plus real-time PCR system (Applied Biosystems) according to the following conditions: 2 min at 50 °C, 10 min at 95 °C, and 40 cycles of 15 s at 95 °C and 1 min at 60 °C using 0.5 µg of cDNA, 2X SYBR Green PCR Master Mix, and 500 nM of the forward and reverse primers. The threshold cycle number (C_T) was calculated with ABI software. Relative transcript quantities were calculated using the $\Delta\Delta C_T$ method [29] with GAPDH as the reference gene amplified from the same samples. The results were expressed as the ratio of reference gene to target gene by using the following formula: $\Delta C_T = C_T$ (Target genes) - C_T (GAPDH). To determine the relative expression levels, the following formula was used: $\Delta\Delta C_T = \Delta C_T$ (Treated) - ΔC_T (Control).The qPCR was performed in triplicate for each experimental group. Normalized fold difference in gene expression is presented graphically to compare the level of transcription.

Table 2
List of primers of the various genes used for real time qPCR analysis.

Sl. No.	Primer Name	Sequence (5′-3′)
1	GAPDH – F	CGGAGTCAACGGATTTGGTC
	GAPDH – R	AGCCTTCTCCATGGTCGTGA
2	Bcl2 – F	ACCTGCACACCTGGATCCA
	Bcl2 – R	AGAGACAGCCAGGAGAAATCAAA
3	Bax – F	AAGCTGAGCGAGTGTCTCCGGCG
	Bax – R	CAGATGCCGGTTCAGGTACTCAGTC
4	Caspase 3 – F	ATACCAGTGGAGGCCGACTTC
	Caspase 3 – R	CAAAGCGACTGGATGAACCA
5	Caspase 9 – F	TGTCCTACTCTACTTTCCCAGGTTTT
	Caspase 9 – R	GTGAGCCCACTGCTCAAAGAT
6	Cathepsin G – F	TCAAGTTTCCTGCCCTGGAT
	Cathepsin G – R	CCTGTGTCCCCGAGAAGAAG
7	Calpain 5 – F	CAGGTCCTCTCAGAGGCAGATAC
	Calpain 5 – R	ACCTCTCCAGGGACCTTAACG
8	Rb1 – F	GAACATCGAATCATGGAATCCCT
	Rb1 – R	AGAGGACAAGCAGATTCAAGGTGAT
9	p-53 – F	GGGTTAGTTTACAATCAGCCACATT
	p-53 – R	GGGCCTTGAAGTTAGAGAAAATTCA
10	Akt 1 – F	GCACAAACGAGGGGAGTACAT
	Akt 1 – R	CCTCACGTTGGTCCACATC
11	MAPK – F	CAATGGCGGTGTGGTGTTC
	MAPK – R	AGCTCCCTTATGATCTGGTTCC
12	JNK – F	TGGACTTGGAGGAGAGAACCA
	JNK – R	CGACGATGATGATGGATGCT
13	IL-1β – F	GCAGCCATGGCAGAAGTACCTGA
	IL-1β – R	CCAGAGGGCAGAGGTCCAGGTC
14	IL-2 – F	CTGCTGGATTTACAGATGATTTA
	IL-2 – R	TGGCCTTCTTGGGCATGT
15	IL-6 – F	CCTGACCCAACCACAAATGC
	IL-6 – R	CCTTAAAGCTGCGCAGAATGA
16	IL-10 – F	CTGGGTTGCCAAGCCTTGT
	IL-10 – R	AGTTCACATGCGCCTTGATG
17	IL-12 – F	CCTGGACCACCTCAGTTTGG
	IL-12 – R	ACGGCCCTCAGCAGGTT
18	IFN-β – F	CTCCTGTTGTGCTTCTCCACT
	IFN-β – R	GGCAGTATTCAAGCCTCCCA
19	IFN-γ – F	CTTTAAAGATGACCAGAGCATCA
	IFN-γ – R	ATCTCGTTTCTTTTTGTTGCTATTGA
20	TNF-α – F	CCCAGGGACCTCTCTCTAATC
	TNF-α – R	ATGGCTACAGGCTTGTCACT
21	Viperin – F	CGTGAGCATCGTGAGCAATG
	Viperin – R	GCTGTCACAGGAGATAGCGA
22	Mx1 – F	CCAGCTGCTGCATCCCACCC
	Mx1 – R	AGGGGCGCACCTTCTCCTCA
23	ISG15 – F	TGGCGGGCAACGAATT
	ISG15 – R	GGGTGATCTGCGCCTTCA
24	**IFITM3 – F**	TCCCACGTACTCCAACTTCCA
	IFITM3 – R	AGCACCAGAAACACGTGCACT

3. Results

3.1. Sequence analysis and characterization using bioinformatics tools

An 81 bp amplicon encoding 27 amino acids was acquired by RT-PCR of cDNA using histone H2A specific primer (Fig. 1A). The PCR products was cloned into pGEM®-T Easy cloning vector and transformed into *E. coli* DH5α competent cells. BLAST analysis of the nucleotide and deduced amino acid sequences of *Fi*-Histin revealed that the peptide belonged to histone H2A family. Homology analysis of *Fi*-Histin nucleotide sequence and deduced amino acid sequence by BLASTn and BLASTp showed that it belongs to the histone H2A sequence of invertebrates. *Fi*-Histin nucleotide sequence showed 100% identity to *F. indicus* (GenBank ID: HM243619.1) and *Ficus gracilis* histone H2A (GenBank ID: HQ720146.1), followed by 99% to *P. monodon* (GenBank ID: HM243620.1) and 94% to *S. scripta* histone H2A (GenBank ID: HQ720149.2). Analysis by ProtParam tool and APD3 predicted a molecular weight of 2.983 kDa, net charge of +6 and a theoretical isoelectric point (pI) of 12.18 respectively. Cationicity of the 27 mer, *Fi*-Histin was primarily due to six positive amino acid residues (Lys (1 No) + Arg (5 Nos)). The estimated half-life of the peptide was predicted to be 1.9 h, > 20 h and > 10 h with respect to mammalian reticulocytes (*in vitro*), yeast (*in vivo*) and *Escherichia coli* (*in vivo*) respectively. Predicted instability index was computed to be 81.89 categorizing the peptide as unstable.

Prediction of antimicrobial activity of *Fi*-Histin by APD3 discovered it as an effective AMP with a protein-binding potential (boman index) and wimley-white whole-residue hydrophobicity of 2.85 kcal/mol and 6.37 kcal/mol respectively. *In silico* analysis based on amphipathicity using HeliQuest tool revealed a hydrophobicity (H) of 0.221 and hydrophobic moment (µH) of 0.269. *Fi*-Histin was found to be rich in Ala (A) 14.8%, Arg (R) 18.5%, 11.1% each of Leu (L), Gly (G) and Ser (S) as in the case of other histone derived AMPs followed by 3.7% each of Asn (N), Gln (Q), His (H), Ile (I), Lys (K), Phe (F), Pro (P), Tyr (Y) and Val (V). Of the total weight of *Fi*-Histin, 55.56% was contributed by polar residues + GLY and 44.44% by nonpolar residues. The helical wheel

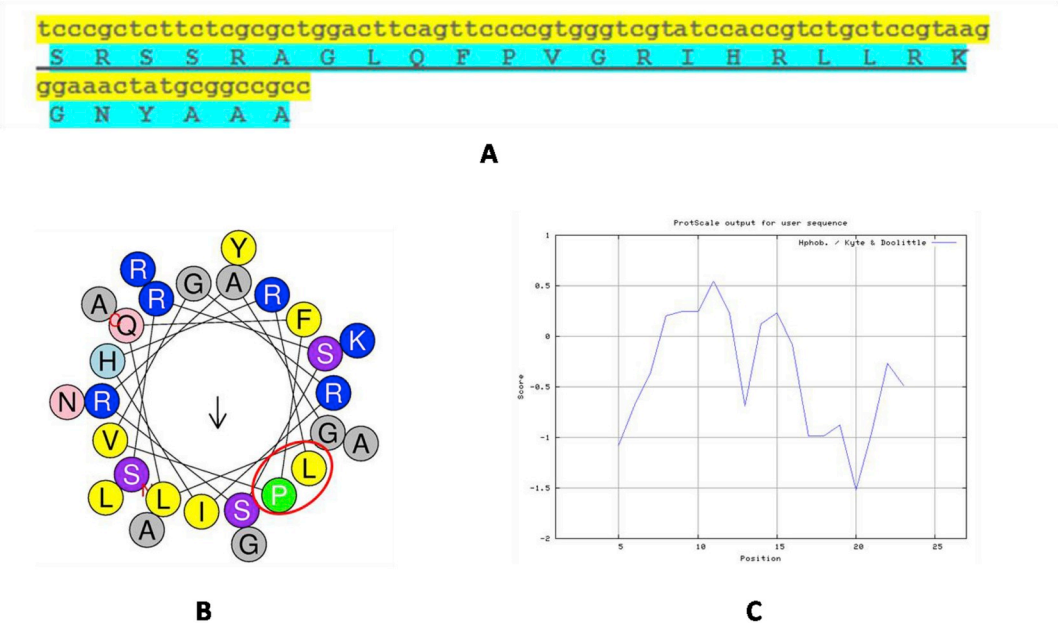

Fig. 1. Nucleotide and deduced amino acid sequence of the HDAP from the haemocyte mRNA transcripts of *F. indicus*–*Fi*-Histin (GenBank ID: KY126319). Underlined region of peptide was synthesized as linear peptide for functional characterization**; B**: The helical wheel diagram of *Fi*-Histin predicted using Heliquest online tool. The structure was built to identify the amphipathicity of the peptide. The amino and carboxy terminal ends are mentioned as N and C, respectively. The expected hydrophobic face LP is shown in the red circle**; C**: Kyte-Doolittle plot showing hydrophobicity of *Fi*-Histin. The peaks above the score (0.0) indicate the hydrophobic nature of the predicted protein. (For interpretation of the references to colour in this figure legend, the reader is referred to the Web version of this article.)

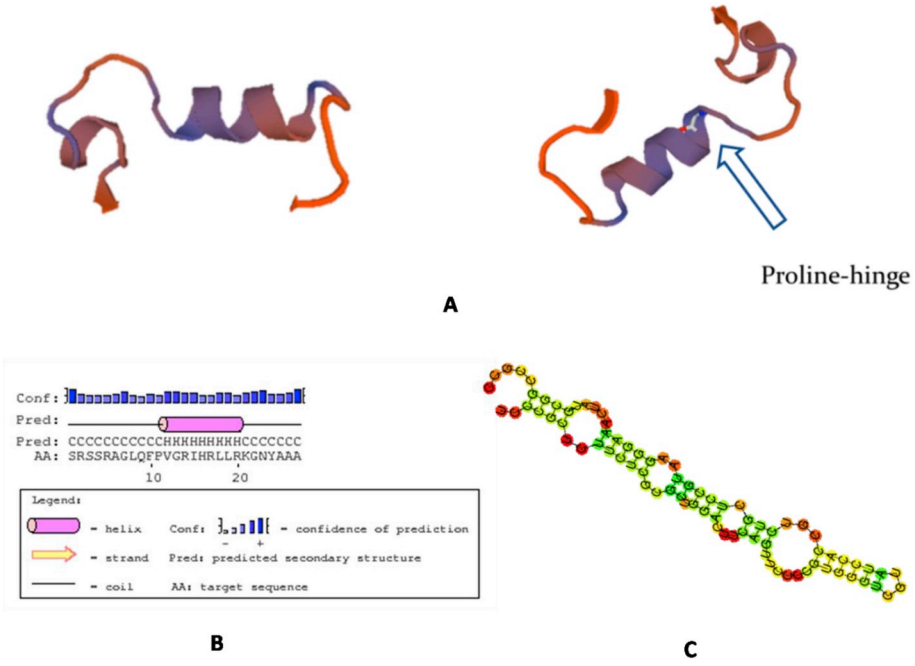

Fig. 2. A: Structural model of *F. indicus*, *Fi*-Histin (GenBank ID: KY126319) created with the PyMol software using the pdb data generated by SWISSMODEL server. **B:** Secondary structure of *Fi*-Histin predicted using PSIPRED server. The α-helix region is shown in pink coloured cylinders and the coiled region is shown in black lines. **C:** Predicted secondary structure of *Fi*-Histin RNA with minimal free energy prediction. (For interpretation of the references to colour in this figure legend, the reader is referred to the Web version of this article.)

obtained depicting the distribution of amino acids based on amphipathicity is presented in Fig. 1B. Hydrophobicity analysis of *Fi*-Histin by Kyte-Doolittle plot (Fig. 1C) confirmed the substantial occurrence of hydrophobic amino acids located in the first 15 residues. Prediction of spatial 3D structure of *Fi*-Histin by homology modelling using the SWISSMODEL sever is given in Fig. 2A and validated the occurrence of an extended α-helix at the N-terminus. Secondary structure prediction using PSIPRED tool revealed the presence of one α-helix in *Fi*-Histin (Fig. 2B). Expected RNA sequence and the secondary structure of *Fi*-Histin with minimum free energy was found to be comprised of paired double stranded and unpaired looped region (Fig. 2C). Bootstrap distance phylogenetic tree constructed using Neighbor-Joining method confirmed the similarity of *Fi*-Histin to the previously reported histone-H2A nucleotide sequences (Fig. 3A). The ClustalW multiple protein sequence alignment of *Fi*-Histin with representatives of histone H2A derived AMPs in BioEdit revealed the existence of conserved sequence features (Fig. 3B).

3.2. Peptide synthesis and molecular characterization

This study represents the first report of a histone, H2A derived AMP from *F. indicus*. In order to characterize the bioactivity, a 21 amino acid

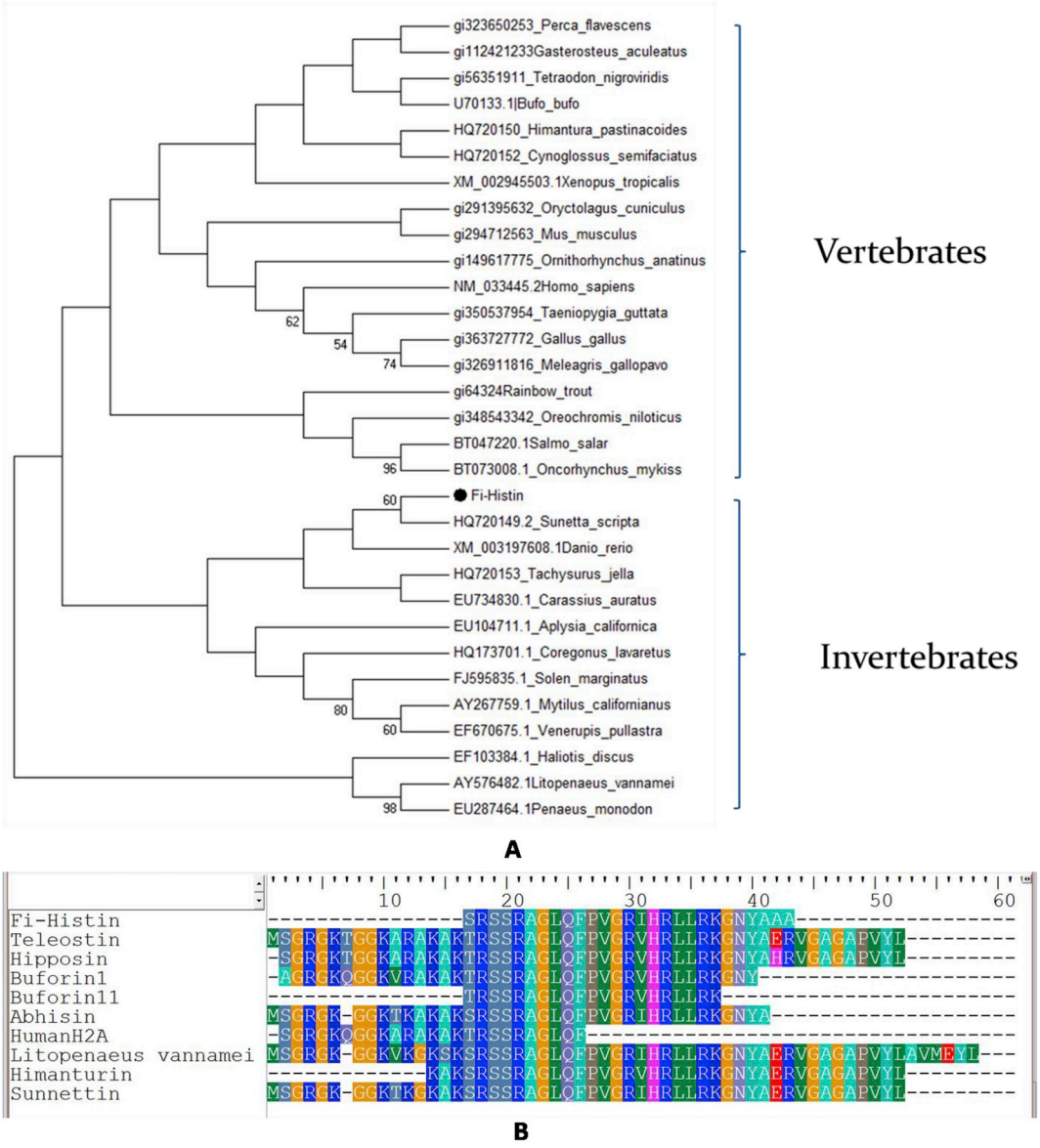

Fig. 3. A: A bootstrapped neighbor-joining tree obtained using MEGA 7 illustrating relationships between the deduced amino acid sequences of the *F. indicus*, *Fi*-Histin (GenBank ID: KY126319) with other histone H2A sequences from vertebrates and invertebrates. Values at the node indicate the percentage of times the particular node occurred in 1000 trees generated by bootstrapping the original deduced protein sequences. Branches corresponding to partitions reproduced in less than 75% bootstrap replicates are collapsed; **B:** Multiple alignment of amino acid sequence of the *Fi*-Histin with other vertebrate and invertebrate H2A sequences obtained using BioEdit. Teleostin (*Tachysurus jella* and *Cynoglossus semifasciatus*), hipposin (*Hippoglossus hippoglossus*), buforin I and II (*Bufo bufo gargarizans*), abhisin (*Haliotis discus*), human H2A, *Litopenaeus vannamei* H2A, *himanturin* (*Himantura pastinacoides*) and *s*unettin (*Sunetta scripta*).

length region of the peptide (**SRSSRAGLQFPVGRIHRLLRK**) sharing similarity to buforin (a histone derived AMP) identified by multiple sequence alignment was selected for solid phase peptide synthesis (Fig. 4A). The synthetic peptide, *Fi*-His_{1-21} is a cationic peptide with a net charge of +6 with a predicted mass and *p*I of 2.428 kDa and 12 respectively. Herein after, the synthetic peptide will be mentioned as *Fi*-His_{1-21}. Synthetic peptide predicted to be an effective AMP with total hydrophobicity of 33%, boman index of 3.34 kcal/mol and wimley-white whole residue hydrophobicity of 3.77 kcal/mol. Peptide cationicity was mainly subsidized by six positively charged residues (Arg (5 Nos) + Lys (1 No)). The helical peptide analysis by Heliquest tool revealed that the hydrophobic and hydrophilic amino acids are clustered on opposite sides and aid in the membrane penetration of peptide with a hydrophobic face of 'Leu and Pro' (LP) (Fig. 4B).

3.3. Determination of molecular mass and purity of synthetic peptide

ESI mass spectroscopy was employed to confirm the molecular weight of synthetic peptide *Fi*-His_{1-21} (2865.28 Da). The ESI mass spectrum of peptide is shown in Fig. 4C. The mass spectrum illustrates the mass to charge ratio (*m/z*) from 400 to 1800 of all the ionized molecules existing in the sample. The most abundant ion in the spectrum is seen at a mass to charge ratio of 955.95. This *m/z* matches to *Fi*-His_{1-21} ionized to +3 (rounded off MW = 2867.85 Da + 3H + = 2870.85). The mass to charge ratio is thus 2870.85/3 = 956.95. The other relatively abundant ion was *m/z* of 717.30 ionized to +4 (round off MW = 2869.2 Da + 4H+ = 2873.2) and thus the *m/z* is 2873.2/4 = 718.3. The peptide was tested for its purity by HPLC and from the chromatogram, it was found to be 95% pure by the percent area of the main peak at retention time 9.183 min as seen in Fig. 4D.

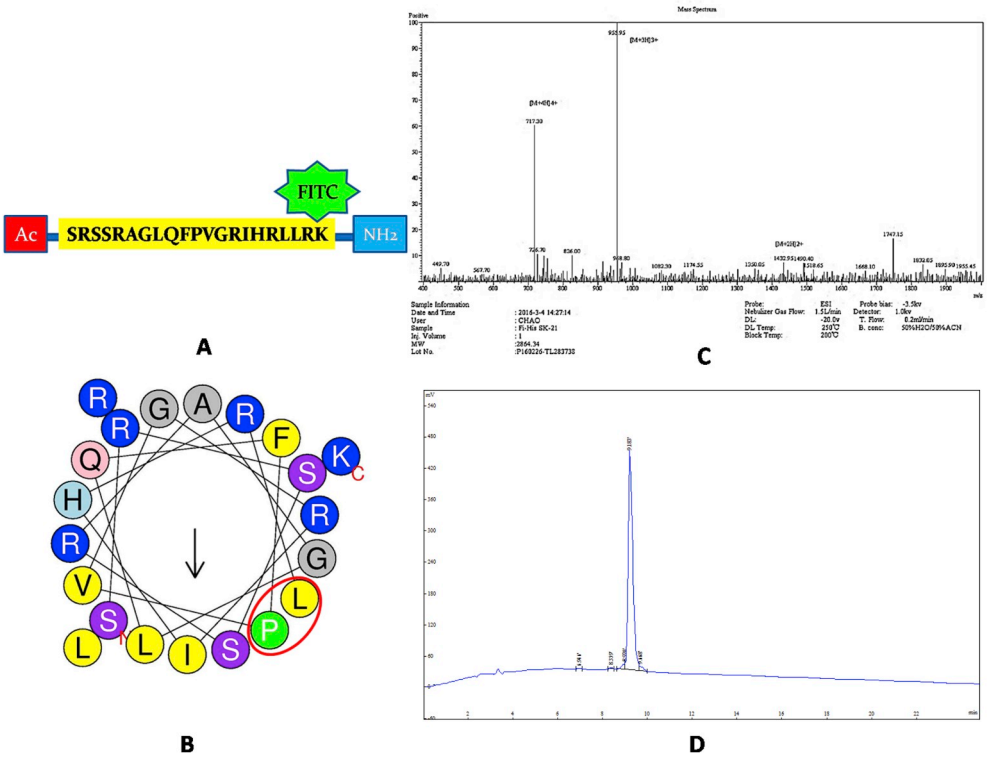

Fig. 4. A: Diagrammatic representation of linear synthetic peptide *Fi*-His$_{1-21}$with N-terminal acetylation (Ac), FITC labeling and C-terminal amidation (NH_2); **B:** The helical wheel diagram of synthetic peptide predicted using Heliquest online tool. The structure was built to identify the amphipathicity of the peptide. The amino and carboxy terminal ends are mentioned as N and C, respectively. The expected hydrophobic face LP is shown in the red circle; **C**: ESI mass spectrum of synthetic peptide, Most abundant ion in spectrum is seen at *m/z* of 955.95 [M + 3H]3 + followed by 717.30 [M + 4H]4 +; **D**: HPLC chromatogram of synthetic peptide showing a major peak at retention time of 9.183 min. (For interpretation of the references to colour in this figure legend, the reader is referred to the Web version of this article).

3.4. Haemolytic activity

Haemolytic activity of synthetic *Fi*-His$_{1-21}$ peptide was tested against human RBCs at different concentrations. As shown in Fig. 5 only about 18% of RBCs were lysed even after the treatment with 400 μM of peptide. Also the peptide was found to be non-haemolytic at the lower concentrations from 100 to 3.125 μM compared to mellitin.

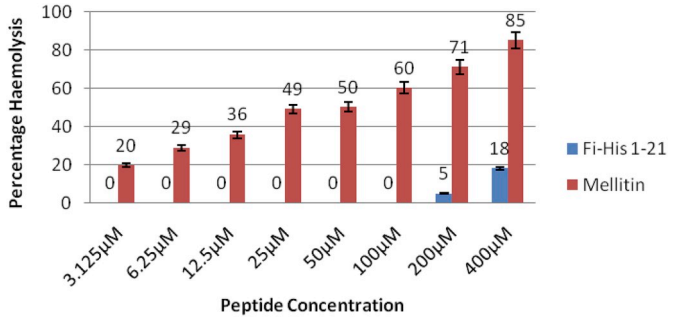

Fig. 5. Haemolytic activity of the synthetic peptide *Fi*-His$_{1-21}$ and the positive peptide control Mellitin in human RBCs at various concentrations.

3.5. Antimicrobial activity

To determine the antimicrobial activity of *Fi*-His$_{1-21}$, the peptide was verified for the capability to inhibit proliferation of microorganisms using MIC and MBC estimation. The result showed that the peptide was active against both Gram-negative and Gram-positive bacteria. Peptide inhibited the growth of *V. vulnificus* with an MIC and MBC of 25 μM each. Against *P. aeruginosa* and *V. parahaemolyticus* the MIC was found to be 25 μM and MBC of 50 μM; for *S. aureus* and *V. cholera* 50 μM was observed to be the MIC value and the MBC value was found to be greater than the highest tested concentration. Bacterial pathogens *E. coli, B. cereus, A. hydrophila, E. tarda* and *V. alginolyticus* were found to be sensitive to *Fi*-His$_{1-21}$, but the MIC and MBC values were found to be > 50 μM. At the highest tested concentration (50 μM), *Fi*-His$_{1-21}$ inhibited the proliferation of *E. coli* by 79%, *B. cereus* by 78%, *A. hydrophila* by 68%, *E. tarda* by 82%, *V. fluvialis* by 85% and *V. alginolyticus* by 89% (Table 3).

Table 3
Antimicrobial activity of synthetic peptide, *Fi*-His$_{1-21}$.

Microorganism	MIC (μM)	MBC (μM)
B. cereus (MCCB 101)	> 50	> 50
S. aureus (MTCC 3061)	50	> 50
E. tarda (MTCC 2400)	> 50	> 50
P. aeruginosa (MCCB 119)	25	50
A. hydrophila (MCCB 113)	> 50	> 50
E. coli (MTCC483)	> 50	> 50
V. cholera (MCCB 129)	50	> 50
V. vulnificus (WV13)	25	25
V. proteolyticus (M10W1)	> 50	> 50
V. alginolyticus (VKF44)	> 50	> 50
V. parahaemolyticus (MCCB 133)	25	50

3.6. Propidium iodide staining

Dead bacterial cells were observed as red in the PI stained image of *Fi*-His$_{1-21}$ treated *V. vulnificus* (Fig. 6A). At the same time, peptide penetrated cells were detected as green because of the presence of FITC tag in the peptide. Thus the images were captured under PI and FITC filter on the same field. Green fluorescencence was observed in bacteria in high numbers showing the internalization of the flourescent peptide into the bacterial cytoplasm.

3.7. SEM analysis

Morphological alterations of *Fi*-His$_{1-21}$ treated *V. vulnificus* were visualized by scanning electron microscopy (SEM) (Fig. 6B). On contrary to smooth surfaced untreated control, *V. vulnificus* cells treated with *Fi*-His$_{1-21}$ was noticed with uneven surface, altered membrane and loss of cytoplasmic content.

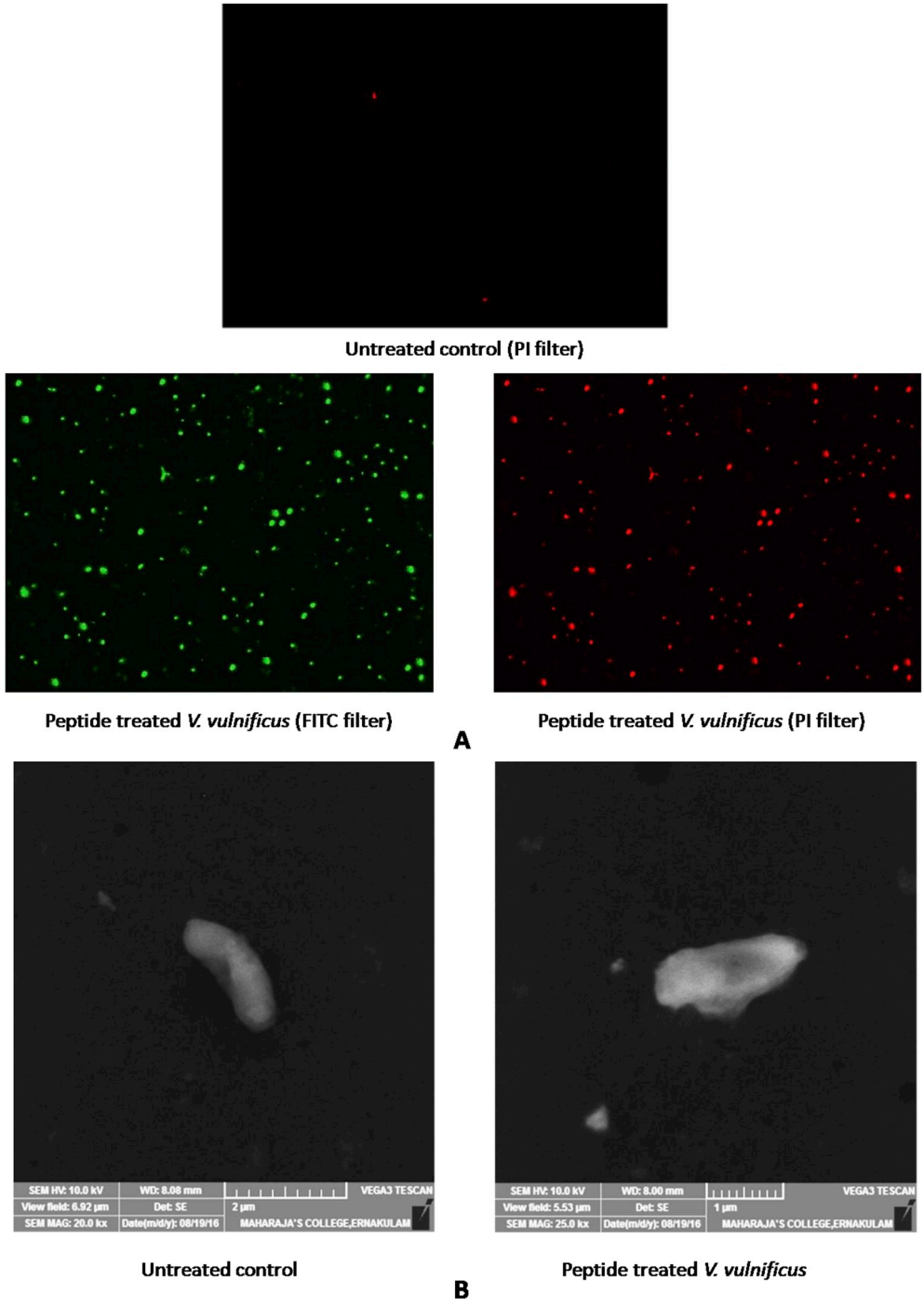

Fig. 6. A: Epifluorescence microscopy images of *V. vulnificus* (control) and synthetic *Fi*-$His_{1\text{-}21}$ peptide treated *V. vulnificus* under FITC filter and PI filter (magnification 100×), stained with Propidium iodide. **B:** Scanning electrom microscope images of *V. vulnificus* (control) and synthetic peptide, *Fi*-$His_{1\text{-}21}$ treated *V. vulnificus* showing the disrupted membrane.

3.8. DNA binding assay

To explore the intracellular targeting mechanisms, the DNA binding affinity of *Fi*-$His_{1\text{-}21}$ was tested by gel retardation assay. For this the electrophoretic moblity of pUC-18 plasmid vector treated with different concentrations of the synthetic *Fi*-$His_{1\text{-}21}$peptide (200 µM–3.125 µM) exhibited notable retardation by DNA binding from a concentration of 200 µM to 12.5 µM (Fig. 7).

3.9. In vitro cytotoxicity assay

Cytotoxicity of *Fi*-$His_{1\text{-}21}$ was tested from 200 µM to 1.625 µM in HEp-2 and NCI–H460 cell lines by XTT assay and the result is represented in Fig. 8. At the highest tested concentration (200 µM), growth inhibition of 94% was exhibited in NCI–H460 and 89% in HEp-2 cell lines. The IC_{50} of *Fi*-$His_{1\text{-}21}$ against HEp-2 cells was estimated to be 31.274 ± 24.531 µM and 22.670 ± 13.939 µM for NCI–H460. *Fi*-

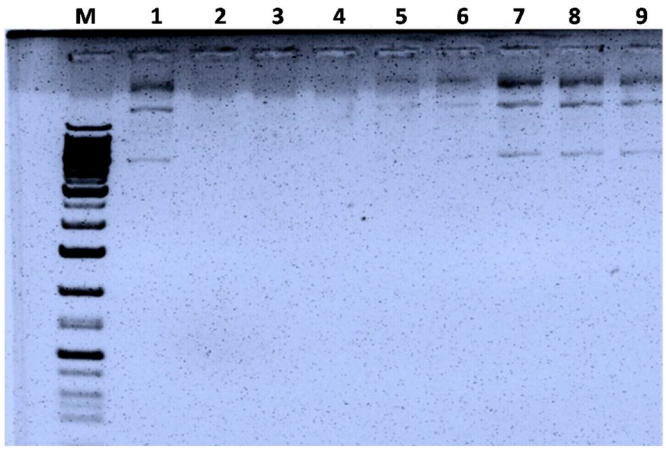

Fig. 7. Agarose gel electrophoretogram of DNA binding assay of synthetic peptide *Fi*-His_{1-21} using pUC-18 vector with various concentrations of peptide. Lane M: 1 kb ladder, Lane 1: Control plasmid, Lane 2–8200 μM–1.652 μM concentration of peptide with 50 ng of pUC-18.

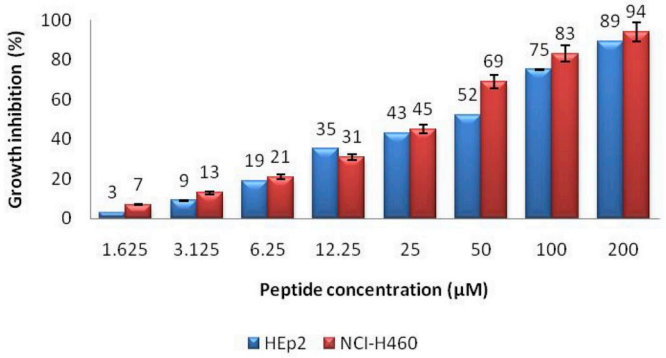

Fig. 8. *In vitro* cytotoxicity of synthetic peptide *Fi*-His_{1-21} in HEp2 and NCI–H460 cells at various tested concentrations'.

His_{1-21} displayed potent cytotoxic activity against HEp-2 and NCI–H460 cell lines and was found to be concentration dependent.

3.10. Anticancer activity

3.10.1. Relative gene expression analysis of cancer related genes in Fi-His_{1-21} treated NCI–H460 lung cancer cells

The *in vitro* gene expression level of cancer related genes in *Fi*-His_{1-21} treated NCI–H460 cell line was analysed by qRT-PCR. Quantitative RT-PCR analysis showed that the relative gene expression of most of the genes was differentially expressed in response to *Fi*-His_{1-21} treatment (Fig. 9A). Most of the genes were noticed to be up-regulated including the cancer controlling genes (Bax, Caspase 3, Caspase 9 and Rb1) and cytokine related immune genes (IFN-b, IFN-c, ISG 15, IFITM3, IL-1β and IL-6).

3.10.2. Relative gene expression analysis of cancer related genes in Fi-His_{1-21} treated HEp-2 pharyngeal cancer cells

The gene expression of cancer controlling and immune related genes in HEp2 cell lines were analysed after peptide treatment by qRT-PCR (Fig. 9B). *Fi*-His_{1-21} treatment in HEp-2 cell lines led to noticeable up-regulation of Bax, TNF-α, Caspase-3, Caspase-9, JNK, Mx-1, IFN-c, ISG15, IFITM3, IL-6, IL-10 and IL-12 and marked down regulation of Bcl2 gene and IL-1β.

4. Discussion

In eukaryotes, histone proteins play an important role in chromatin packaging and can also turn as antimicrobials by involving in the host defense processes against infection [30]. The present study reports a histone derived AMP, *Fi*-Histin from *F. indicus*. Molecular characterization of the peptide was done and functional characterization of the synthetic *Fi* $His_{1-21}$was carried out.

Multiple sequence alignment (ClustalW) of *Fi*-Histin with other reported HDAPs revealed the existence of conserved residues. While considering the differences, *Fi*-Histin showed a hydrophilic amino acid 'Ser' residue at N-terminus region when compared to other HDAPs from vertebrates where, hydrophilic 'Thr' is present in the place. Also in *Fi*-Histin at 15^{th} amino acid from N-terminus is a hydrophobic amino acid 'Ile', which is same for all other invertebrate HDAPs; but replaced by hydrophobic 'Val' in all vertebrate HDAPs. Phylogenetic tree of *Fi*-Histin constructed based on amino acid sequences of previously reported histone H2A derived AMPs validates that the HDAPs are derived from a common ancestor by sequences of evolutionary modifications. The invertebrate HDAPs and vertebrate HDAPs formed a separate group. Compared to other AMPs, HDAP genes evolve very slowly and thus evolutionary studies are of immense importance [31]. Sequence and structural analysis revealed *Fi*-Histin as an amphipathic and alpha helical cationic AMP with similarity to other known histone H2A derived AMPs [11,32]. Antimicrobial action of α-helical cationic peptides has been anticipated to arise through three general mechanisms: binding to the cell surface, microbial membrane permeabilization and secondary effects including DNA/protein binding, membrane compositional rearrangements, interference with essential cellular machinery, etc [33,34]. In addition to membrane disruption antimicrobial mechanism of HDAPs also includes interactions with nucleic acids [35,36].

Based on the multiple sequence alignment data from *Fi*-Histin, a 21 amino acid region was selected based on the similarity to buforin II and named as *Fi*-His_{1-21}. Peptide was synthesized as linear peptide with end modifications and an FITC-tag. Previous study of anticancer activity of buforin II with FITC labelling showed that FITC-labelling had no adverse effects on the cytotoxicity of the peptides when compared to peptide without labelling [19]. *Fi*-His_{1-21} has a net charge of +6 with molecular weight of 2.428 kDa, hydrophobicity of 33%, and *p*I of 12, making it highly positively charged in physiological media. Birkemo et al. [24] and Chen et al. [37] reported that increased hydrophobicity of the peptide to a certain extent increases the antimicrobial activity. Pasupuleti et al. [38] reported that the net charge above a threshold maximum may not increase the antimicrobial activity since the robust interactions with phospholipid head groups, prevents structuring and further translocation of the peptide.

Similar to the buforin II, *Fi*-His_{1-21} is also a cationic α-helical peptide. Main difference in amino acid sequence to buforin II is in two amino acids, 'Ser' in first position is replaced by 'Thr' and 'Ile' at 15th place by 'Val' in buforin II. Yi et al. [39] elucidated the structure of buforin II using NMR spectroscopy and found that it adopts a helix-hinge-helix; with an N-terminal extended α-helix from Arg_5 to Phe_{10}, and the C-terminal α-helix encompassing residues from Val_{12} to Lys_{21}. *Fi*-Histin also exhibits the same structural features including the 'Pro_{11}' hinge between the two helices. Kobayashi et al. [40] investigated about the role of Pro in interaction with membrane system and found that Pro_{11} distorts the helical structure of buforin II and forms a hinge like structure, conferring the unique cell penetrating property. Later in 2004, Kobayashi et al. [41] found that translocation of peptide, buforin II was by toroidal pore formation. Microbicidal activity and the anticancer activity of buforin II has been reported by various scientists due to the intracellular nucleic acid binding especially with DNA and RNA [11,18,42].

Antimicrobial activity of histone H2A derived AMPs against both Gram-positive and Gram-negative bacteria especially drug resistant pathogens and fungi were described by several scientists

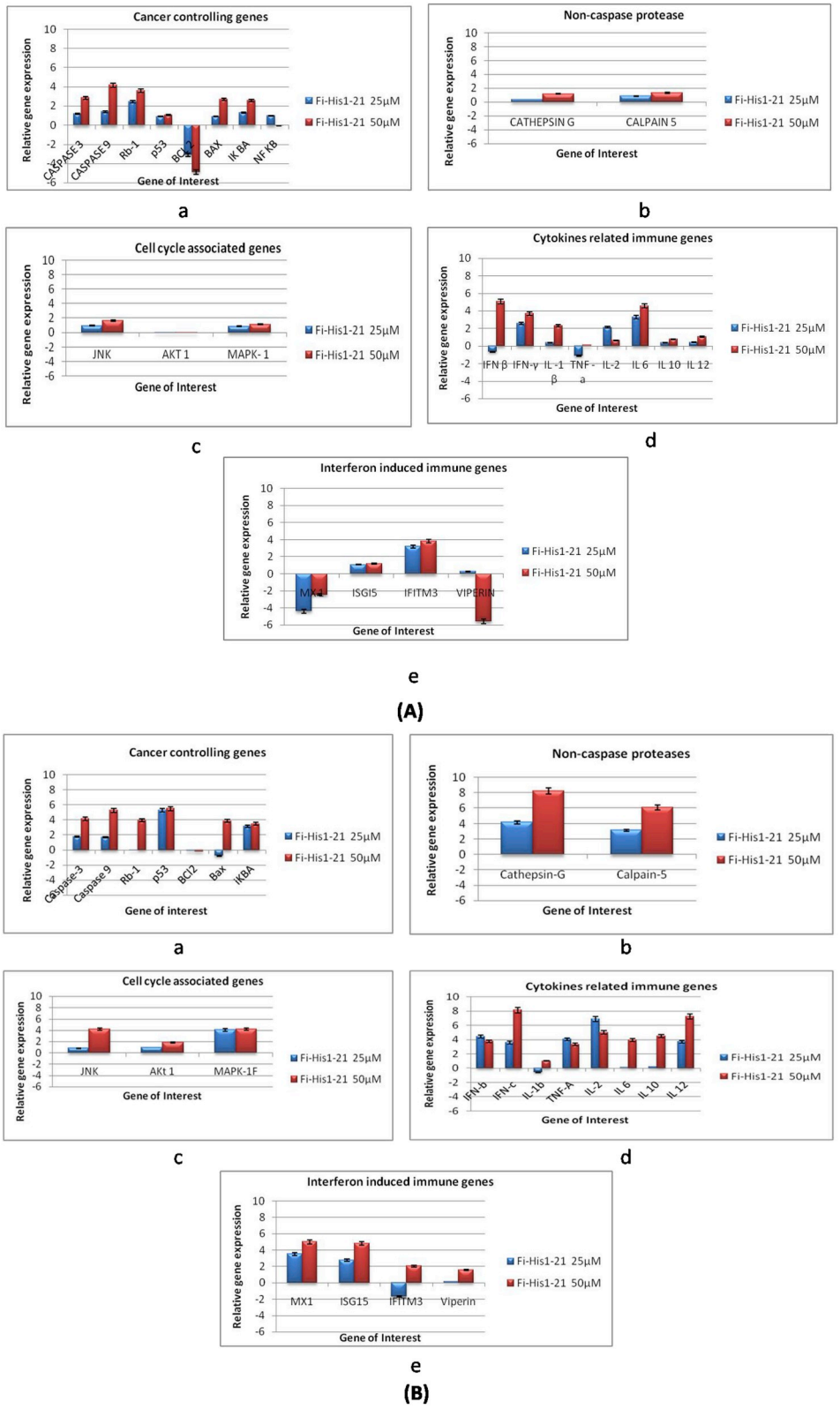

Fig. 9. Relative gene expression profile of different cancer related genes using real time PCR and the $\Delta\Delta C_T$ method in peptide treated cell lines **A(a-e):** NCI–H460 cell lines; **B (a–e):** HEp-2 cell lines.

[10,24,43–46]. The antimicrobial activity showed by synthetic *Fi*-His$_{1-21}$ was in agreement with the previously reported HDAPs such as hipposin, parasin I, buforin I and buforin II. Like other HDAPs, *Fi*-His$_{1-21}$ also exhibited broad spectrum antibacterial activity against Gram-positive and Gram-negative bacteria which includes both aquatic and human pathogens. Activity of *Fi*-His$_{1-21}$ was observed to be dose dependent and antimicrobial activity was detected down to a concentration of 1.625 µM. At the lowest tested concentration (1.625 µM), the peptide was found to inhibit the growth of Gram-positive bacteria *S. aureus* by 59% and that of *B. cereus* by 62%.

Most of the tested pathogens were found to be sensitive against *Fi*-His_{1-21}. Microbicidal activity of the peptide was confirmed by plating the peptide treated bacteria in the LB agar plates and the MBC was found to be 25 μM for *V. vulnificus*. The bactericidal activity was further analysed by epifluorescence microscopy after staining using permeability marker, PI and the dead cells were observed as red indicating that the bacterial membrane is permeabilized. Morphological variations in peptide treated *V. vulnificus* were observed through SEM in order to better understand the mode of microbicidal activity and membrane perturbed bacteria without any blebbing or pores compared to untreated control clearly observed in the SEM image. Like other reported HDAPs, the cationic nature of *Fi*-His_{1-21}could assist in the antimicrobial action *via* electrostatic interaction with microbial membranes. Chen et al. [17] observed the LPS and LTA binding activity of H2A N-terminus derived AMP, Sphistin from *S. paramamosain* and speculated that the electrostatic attraction to negatively charged microbial surfaces is involved in the initial stage of antimicrobial mechanism. The α-helical nature of *Fi*-His_{1-21} could attach to the microbial membrane with partitioning of hydrophilic and hydrophobic amino acids followed by interaction with the phospholipid bilayer of microbe. Epifluorescence microscopy image of *V. vulnificus* treated with peptide appeared fluorescent (green) through FITC filter which ensures the entry of peptide. SEM investigation revealed the cell membrane rupture and cell content leakage inferring that the killing could be *via* initial binding followed by permeabilization and cell damage.

DNA binding activity of buforin II and buforin III revealed that antimicrobial activity is correlated with DNA binding affinity of the peptide [42,47]. Synthetic *Fi*-His_{1-21} exhibited a remarkable DNA binding activity even at 12.5 μM, which is a lower concentration than the MIC. Thus with the α-helical content, cationicity and hydrophobicity the DNA binding activity of synthetic *Fi*-His_{1-21} augments the antimicrobial activity. Previous studies revealed that the synthetic and purified N-terminal region of histone H2A derived AMPs exhibited antimicrobial and anticancer activity [11,13,14,17,24,48].

Recently, anticancer peptides (ACPs) gained consideration as a substitute to chemotherapeutic drugs. ACPs have benefits over currently used anticancer therapeutics, by virtue of its potential in discriminating normal and cancer cells and ability to circumvent the multidrug-resistance mechanism [49]. HDAPs including buforin IIb were found to be non-cytotoxic to normal cells [47]. Anticancer activity of HDAP, buforin IIb was studied by Lee et al. [19] and found that the cytotoxic activity against cancer cells were mainly by directing cancer cells through interaction with cell surface gangliosides, phosphatidylserine (PS) and heparin sulfate (HS). Without damaging the cell membrane, the peptide induced apoptosis *via* intrinsic pathway mediated through induction of caspase-3 and caspase-9. Anticancer mechanism by *Fi*-His_{1-21} in NCI–H460 and HEp-2 cell lines was observed by gene expression analysis using qRT-PCR. Our results propose that *Fi*-His_{1-21} up-regulates apoptosis related to caspase-3 and caspase-9 activation in both the tested cell lines. Apparently, this could be resulted from the release of cytochrome *c* from mitochondria which in turn get activated downstream caspase-9 and caspases-3. The linear peptide *Fi*-His_{1-21} induced the activation of caspase-9, which could initiates mitochondrion-dependent apoptosis. In both the cell lines, the up-regulation of analysed caspases was found to be concentration dependent [50]. Mitochondria dependent mode of apoptosis induction is involved in the anticancer activity of most of the AMPs. The AMPs such as RGD-tachyplesin, buforin IIb and DP1 were also observed to persuade apoptosis in tumour cells *via* mitochondrion-dependent pathway [51].

The up-regulation of mRNA of pro-apoptotic protein Bax and further down-regulation of anti-apoptotic protein Bcl2 was observed in both the cell lines, and the ratio of Bax: Bcl2 proteins is believed to get augmented upon apoptosis induction [52]. The tumour suppressor genes p53 and Rb1 which aid in the regulation of cell growth and cell division were also found to be up-regulated followed by peptide treatment in both cell lines. Similar kind of up-regulation of p53 mRNA was noticed in epinecidin-1 treated U-937 leukaemia cell lines [53]. Expression level of non-caspase proteases, Cathepsin-G and Calpain-5 were also high in both cell lines. Both the proteases expressed significantly in NCI–H460 cells compared to HEp-2 upon peptide treatment. Thus along with other caspases, these non-caspase proteases could also assist in the apoptosis.

The pattern of gene expression level of MAPKs, MAPK1 and JNK were found to be up-regulated after peptide treatment in both cell lines. Thus the induction could lead to the phosphorylation of substrates involved in different signalling pathways for apoptosis induction, augmenting the anticancer activity of *Fi*-His_{1-21} peptide. While analysing the relative mRNA level of cytokine genes in both cell lines after *Fi*-His_{1-21}treatment, induction of all tested interleukins, TNF-α and that of interferons, IFN-α and IFN-γ have been detected. Similar kind of induction of cytokines was observed after administration of pardaxin peptide in HeLa cell lines [54]. Up-regulated gene expression of pro-inflammatory cytokines, such as TNF-α and IL-6 proposed a possible increase in phagocytosis as in the case of peptide, TH 1–5 treated HT1080 cell lines [55]. Interestingly, the peptide exhibited anti-cancer activity along with immunomodulatory activity in both the tested cell lines identical to other ACPs such as buforin II, epinecidin-1, S-ALF, pardaxin and Tilapia hepcidins (TH1-5) [51,53–55]. In the development of novel antimicrobials as drug, the main hurdle is the cytotoxicity against host cells. Majority of the HDAPs are found to be non-cytotoxic to normal eukaryotic cells including buforin IIb [19] and Sphistin [17]. Likewise, *Fi*-His_{1-21} was also found to be non-cytotoxic against mammalian erythrocytes through a haemolytic assay. Synthetic HDAP, abhisin exhibited cytotoxicity against leukemia cancer (THP-1) cells, but not for normal fibroblast vero cells [13], similarly *Fi*-His_{1-21} also displayed anticancer activity against cancer cell lines including lung cancer (NCI–H460) cells and pharyngeal cancer (HEp-2) cells without cytotoxicity against human RBCs in haemolytic assays.

5. Conclusion

In conclusion, a histone derived antimicrobial peptide; *Fi*-Histin was identified and cloned from haemocytes of Indian white shrimp, *F. indicus*. The synthetic peptide, *Fi*-His_{1-21} exhibited broad spectrum antimicrobial activity and remarkable anticancer activity with low toxicity towards human erythrocytes. Further studies are needed to elucidate the exact mode of anticancer activity exhibited by the synthetic *Fi*-His_{1-21} peptide. In recent years the contribution of AMPs to host defense mechanisms and their potential as new pharmaceutical substances is becoming increasingly appreciated. This is mainly because of the broad spectrum activity of AMPs and the rapid development of microbial resistance to conventional antibiotics. Thus the peptide *Fi*-His_{1-21} is a prospective contender for preclinical studies for its application as a therapeutic drug against bacterial infections and in cancer therapy.

Conflicts of interest

Sruthy K. S., Aishwarya Nair, Swapna P. Antony, Jayesh Puthumana, I. S. Bright Singh and Rosamma Philip declare that they have no conflict of interest.

Ethical approval

“Not required”.

Funding

The study was funded by Ministry of Earth Sciences (MoES), Govt. of India (MoES/10-MLR/01/2012).

Acknowledgement

The authors are grateful to the Director, Centre for Marine Living Resources and Ecology (CMLRE) and Ministry of Earth Sciences, Govt. of India for the research grant (MoES/10-MLR/01/2012) and scientific support for the work. Authors also thank Coordinator, National Centre for Aquatic and Animal Health (NCAAH) for scientific support. The first author gratefully acknowledges KSCSTE (Kerala State Council for Science, Technology and Environment) for the award of fellowship.

References

[1] R.E.W. Hancock, A. Patrzykat, Clinical development of cationic antimicrobial peptides: from natural to novel antibiotics, Curr. Drug Targets - Infect. Disord. 2 (2002) 79–83.
[2] L.T. Nguyen, E.F. Haney, H.J. Vogel, The expanding scope of antimicrobial peptide structures and their modes of action, Trends Biotechnol. 29 (2011) 464–472, https://doi.org/10.1016/j.tibtech.2011.05.001.
[3] J.M. Conlon, Host-defense peptides of the skin with therapeutic potential: from hagfish to human, Peptides 67 (2015) 29–38, https://doi.org/10.1016/j.peptides.2015.03.005.
[4] R. Sinha, P. Shukla, Antimicrobial Peptides: Recent Insights on Biotechnological Interventions and Future Perspectives, Protein Peptide Lett., 2018, https://doi.org/10.2174/0929866525666181026160852.
[5] H.G. Boman, Antibacterial Peptides : Basic Facts and Emerging Concepts, (2003), pp. 197–215.
[6] M.H. Parseghian, K.A. Luhrs, Beyond the walls of the nucleus: the role of histones in cellular signaling and innate immunity, Biochem. Cell Biol. 84 (2006) 589–604.
[7] J.J. Wyrick, M.A. Parra, The role of histone H2A and H2B post-translational modifications in transcription: a genomic perspective, Biochem. Biophys. Res. Commun. 1789 (2009) 37–44.
[8] C. Tagai, S. Morita, T. Shiraishi, K. Miyaji, S. Iwamuro, Antimicrobial properties of arginine- and lysine-rich histones and involvement of bacterial outer membrane protease T in their differential mode of actions, Peptides 32 (2011) 2003–2009.
[9] H.S. Kim, C.B. Park, M.S. Kim, S.C. Kim, cDNA cloning and characterization of buforin I, an antimicrobial peptide: a cleavage product of histone H2A, Biochem. Biophys. Res. Commun. 229 (1996) 381–387.
[10] C.B. Park, M.S. Kim, S.C. Kim, A novel antimicrobial peptide from Bufobufogargarizans, Biochem. Biophys. Res. Commun. 218 (1996) 408–413.
[11] C.B. Park, H.S. Kim, S.C. Kim, Mechanism of action of the antimicrobial peptide buforin II: buforin II kills microorganisms by penetrating the cell membrane and inhibiting cellular functions, Biochem. Biophys. Res. Commun. 244 (1998) 253–257, https://doi.org/10.1006/bbrc.1998.8159.
[12] C. Li, L. Song, J. Zhao, L. Zhu, H. Zou, Preliminary study on a potential antibacterial peptide derived from histone H2A in hemocytes of scallop Chlamysfarreri, Fish Shellfish Immunol. 22 (2007) 663–672, https://doi.org/10.1016/j.fsi.2006.08.013.
[13] M. De Zoysa, C. Nikapitiya, I. Whang, J. Lee, J. Lee, Abhisin , A potential antimicrobial peptide derived from histone H2A of disk abalone (Haliotis discus discus), Fish Shellfish Immunol. 27 (2009) 639–646, https://doi.org/10.1016/j.fsi.2009.08.007.
[14] S.A. Patat, R.B. Carnegie, C. Kingsbury, P.S. Gross, R. Chapman, K.L. Schey, Antimicrobial activity of histones from hemocytes of the pacific white shrimp, Eur. J. Biochem. 271 (2004) 4825–4833.
[15] J. Arockiaraj, A.J. Gnanam, V. Kumaresan, R. Palanisamy, P. Bhatt, M.K. Thirumalai, et al., An unconventional antimicrobial protein histone from freshwater prawn Macrobrachiumrosenbergii: analysis of immune properties, Fish Shellfish Immunol. 35 (2013) 1511–1522.
[16] M.K. Chaurasia, R. Palanisamy, P. Bhatt, V. Kumaresan, A.J. Gnanam, M. Pasupuleti, et al., A prawn core histone 4: derivation of N- and C-terminal peptides and their antimicrobial properties, molecular characterization and mRNA transcription, Microbiol. Res. 170 (2015) 78–86.
[17] B. Chen, D.Q. Fan, K.X. Zhu, Z.G. Shan, F.Y. Chen, L. Hou, L. Cai, K.J. Wang, Mechanism study on a new antimicrobial peptide Sphistin derived from the N-terminus of crab histone H2A identified in haemolymphs of Scylla paramamosain, Fish Shellfish Immunol. 47 (2015) 833–846, https://doi.org/10.1016/j.fsi.2015.10.010.
[18] J.H. Cho, B.H. Sung, S.C. Kim, Buforins: histone H2A-derived antimicrobial peptides from toad stomach, Biochim. Biophys. Acta 1788 (2009) 1564–1569, https://doi.org/10.1016/j.bbamem.2008.10.025.
[19] H.S. Lee, C.B. Park, J.M. Kim, S.A. Jang, I.Y. Park, M.S. Kim, et al., Mechanism of anticancer activity of buforinIIb, a histone H2A-derived peptide, Cancer Lett. 271 (2008) 47–55.
[20] S.P. Antony, I.S.B. Singh, R. Philip, Molecular characterization and phylogenetic analysis of a penaeidin-like antimicrobial peptide, Fi-penaeidin from Fenneropenaeusindicus, Aquaculture 319 (2011) 298e301 https://doi.org/10.1016/j.aquaculture.2011.06.011.
[21] K.S. Sruthy, A. Nair, J. Puthumana, S.P. Antony, I.S.B. Singh, R. Philip, Molecular cloning, recombinant expression and functional characterization of an antimicrobial peptide, Crustin from the Indian white shrimp, Fenneropenaeusindicus, Fish Shellfish Immunol. 71 (2017) 83–94, https://doi.org/10.1016/j.fsi.2017.09.071.
[22] S.P. Antony, I.S.B. Singh, R. Philip, Molecular characterization and phylogenetic analysis of a penaeidin-like antimicrobial peptide, Fi-penaeidin from Fenneropenaeusindicus, Aquaculture 319 (2011) 298–301, https://doi.org/10.1016/j.aquaculture.2011.06.011.
[23] V.V. Afsal, S.P. Antony, R. Philip, I.S. Bright Singh, Molecular characterization of a newly identified subfamily member of penaeidin from two penaeid shrimps, fenneropenaeusindicus and metapenaeusmonoceros, probiotics antimicrob, Proteins 8 (2016) 46–52, https://doi.org/10.1007/s12602-015-9203-9.
[24] G.A. Birkemo, T. Lüders, Ø. Andersen, I.F. Nes, J. Nissen-Meyer, Hipposin, a histone-derived antimicrobial peptide in Atlantic halibut (Hippoglossushippoglossus L.), Biochim. Biophys, Acta - Proteins Proteomics 1646 (2003) 207–215, https://doi.org/10.1016/S1570-9639(03)00018-9.
[25] Y. Onuma, M. Satake, T. Ukena, J. Roux, S. Chanteau, N. Rasolofonirina, M. Ratsimaloto, H. Naoki, T. Yasumoto, Identification of putative palytoxin as the cause of clupeotoxism, Toxicon 37 (1999) 55–65.
[26] R.S. Miles, S.G.B. Amyes, Laboratory control of antimicrobial therapy, in: J.G. Collee, A.G. Fraser, B.P. Marmion, A.G. Simmons (Eds.), Practical Medical Microbiology, Churchill Iivingstone, New York, 1996.
[27] J. Andrä, J. Howe, P. Garidel, M. Rössle, W. Richter, J. Leiva-León, I. Moriyon, R. Bartels, T. Gutsmann, K. Brandenburg, Mechanism of interaction of optimized Limulus-derived cyclic peptides with endotoxins: thermodynamic, biophysical and microbiological analysis, Biochem. J. 406 (2007) 297–307, https://doi.org/10.1042/BJ20070279.
[28] CLSI, Performance Standards for Antimicrobial Disk Susceptibility Tests, Approved Standard, CLSI Document M02-A11, seventh ed., Clinical and Laboratory Standards Institute, Wayne, Pennsylvania 19087, USA, 2012950 West Valley Road, Suite 2500.
[29] K.J. Livak, T.D. Schmittgen, Analysis of relative gene expression data using real-time quantitative PCR and the 2 ⧖ ⌬⌬ C T method, Methods 25 (2001) 402–408, https://doi.org/10.1006/meth.2001.1262.
[30] A. Patrzykat, L. Zhang, V. Mendoza, G.K. Iwama, R.E. Hancock, Synergy of histone-derived peptides of coho salmon with lysozyme and flounder pleurocidin, Antimicrob. Agents Chemother. 45 (2001) 1337–1342.
[31] T.H. Thatcher, M.A. Gorovsky, Phylogenetic analysis of the core histones H2A, H2B, H3, and H4, Nucleic Acids Res. 22 (1994) 174–179.
[32] N. Sathyan, R. Philip, E.R. Chaithanya, P.R. Anil Kumar, S.P. Antony, Identification of a histone derived, putative antimicrobial peptide Himanturin from round whip ray Himantura pastinacoides and its phylogenetic significance, Results Immunol. 2 (2012) 120–124, https://doi.org/10.1016/j.rinim.2012.06.001.
[33] M. Dathe, T. Wieprecht, Structural features of helical antimicrobial peptides: their potential to modulate activity on model membranes and biological cells, Biochim. Biophys. Acta 1462 (1999) 71–87.
[34] A. Giangaspero, L. Sandri, A. Tossi, Amphipathic α helical antimicrobial peptides, Eur. J. Biochem. 268 (2001) 5589–5600.
[35] Y.S. Koo, J.M. Kim, I.Y. Park, B.J. Yu, S.A. Jang, K.S. Kim, C.B. Park, J.H. Cho, S.C. Kim, Structure-activity relations of parasin I, a histone H2A-derived antimicrobial peptide, Peptides 29 (2008) 1102–1108, https://doi.org/10.1016/j.peptides.2008.02.019.
[36] M.E. Bustillo, A.L. Fischer, M.A. Labouyer, J.A. Klaips, A.C. Webb, D.E. Elmore, Modular analysis of hipposin, a histone-derived antimicrobial peptide consisting of membrane translocating and membrane permeabilizing fragments, Biochim. Biophys. Acta Biomembr. 1838 (2014) 2228–2233, https://doi.org/10.1016/j.bbamem.2014.04.010.
[37] Y. Chen, M.T. Guarnieri, A.I. Vasil, M.L. Vasil, C.T. Mant, R.S. Hodges, Role of peptide hydrophobicity in the mechanism of action of alpha-helical antimicrobial peptides, Antimicrob, Agents Chemother. 51 (2007) 1398–1406.
[38] M. Pasupuleti, A. Schmidtchen, M. Malmsten, Antimicrobial peptides: key components of the innate immune system, Crit. Rev. Biotechnol. 32 (2012) 143–171.
[39] G.S. Yi, C.B. Park, S.C. Kim, C. Cheong, Solution structure of an antimicrobial peptide buforin II, FEBS Lett. 398 (1996) 87–90.
[40] S. Kobayashi, K. Takeshima, C.B. Park, S.C. Kim, K. Matsuzaki, Interactions of the novel antimicrobial peptide buforin 2 with lipid bilayers: proline as a transloca- tion promoting factor, Biochemistry 39 (2000) 8648–8654.
[41] S. Kobayashi, A. Chikushi, S. Tougu, Y. Imura, M. Nishida, Y. Yano, K. Matsuzaki, Membrane translocation mechanism of the antimicrobial peptide buforin 2, Biochemistry 43 (2004) 15610–15616.
[42] E.T. Uyterhoeven, C.H. Butler, D. Ko, D.E. Elmore, Investigating the nucleic acid interactions and antimicrobial mechanism of buforin II, FEBS Lett. 582 (2008) 1715–1718.
[43] C.B. Park, K.S. Yi, K. Matsuzaki, M.S. Kim, S.C. Kim, Structure–activity analysis of buforin II, a histone H2A-derived antimicrobial peptide: the proline hinge is responsible for the cell-penetrating ability of buforin II, Proc. Natl. Acad. Sci. U. S. A 97 (2000) 8245–8250.
[44] A. Giacometti, O. Cirioni, M.S. Del Prete, A.M. Paggi, M.M. D'Errico, G. Scalise, Combination studies between polycationic peptides and clinically used antibiotics against Gram-positive and Gram-negative bacteria, Peptides 21 (2000) 1155–1160.
[45] A. Giacometti, O. Cirioni, M.S. Del Prete, F. Barchiesi, A. Fineo, G. Scalise, Activity of buforin II alone and in combination with azithromycin and minocycline against *Cryptosporidium parvum* in cell culture, J. Antimicrob. Chemother. 47 (2001) 97–99.
[46] R.C. Richards, D.B. O'Neil, P. Thibault, K.V. Ewart, Histone H1: an antimicrobial protein of Atlantic salmon (Salmosalar), Biochem. Biophys. Res. Commun. 284 (2001) 549–555.
[47] S.A. Jang, H. Kim, J.Y. Lee, J.R. Shin, D.J. Kim, J.H. Cho, S.C. Kim, Mechanism of action and specificity of antimicrobial peptides designed based on buforinIIb, Peptides 34 (2012) 283–289, https://doi.org/10.1016/j.peptides.2012.01.015.
[48] G. Bergsson, B. Agerberth, H. Jornvall, G.H. Gudmundsson, Isolation and identification of antimicrobial components from the epidermal mucus of Atlantic cod

(Gadusmorhua), FEBS J. 272 (2005) 4960e4969.
[49] N. Papo, Y. Shai, Host defense peptides as new weapons in cancer treatment, Cell. Mol. Life Sci. 62 (2005) 784–790.
[50] S.H. Kaufmann, W.C. Earnshaw, Induction of apoptosis by cancer chemotherapy, Exp. Cell Res. 256 (2000) 42–49.
[51] M.C. Lin, S.B. Lin, J.C. Chen, C.F. Hui, J.Y. Chen, Shrimp anti-lipopolysaccharide factor peptide enhances the antitumor activity of cisplatin in vitro and inhibits HeLa cells growth in nude mice, Peptides 31 (2010) 1019–1025, https://doi.org/10.1016/j.peptides.2010.02.023.
[52] L.K. Leung, T.T.Y. Wang, Differential effects of chemotherapeutic agents on the Bcl-2/Bax apoptosis pathway in human breast cancer cell line MCF-7, Breast Canc. Res. Treat. 55 (1999) 73–83.
[53] J.-Y. Chen, W.-J. Lin, J.-L. Wu, G.M. Her, C.-F. Hui, Epinecidin-1 peptide induces apoptosis which enhances antitumor effects in human leukemia U937 cells, Peptides 30 (2009) 2365–2373, https://doi.org/10.1016/j.peptides.2009.08.019.J.C.
[54] L.C. Hsu, J.T.C. Tzen, J.Y. Chen, Pardaxin-induced apoptosis enhances antitumor activity in HeLacells, Peptides 32 (2011) 1110–1116, https://doi.org/10.1016/j.peptides.2011.04.024.
[55] W.-T. Chang, C.-Y. Pan, V. Rajanbabu, C.-W. Cheng, J.-Y. Chen, Tilapia *(Oreochromis mossambicus)* antimicrobial peptide, hepcidin 1-5, shows antitumor activity in cancer cells, Peptides 32 (2011) 342–352, https://doi.org/10.1016/j.peptides.2010.11.003.